Joint Subaru/Gemini Science Conference 2009

The stellar populations of Lyman Break Galaxies at z~5 in the GOODS-N

K. Yabe, K. Ohta (Kyoto Univ.), I. Iwata (NAO, Okayama), M. Sawicki (St. Mary's Univ.), N. Tamura, K. Aoki (NAO, Hawaii), M. Akiyama, T. Ichikawa, M. Kajisawa (Tohoku Univ.), and MOIRCS team

Abstract

We present the results of SED fitting analysis for Lyman Break Galaxies at z~5 in the GOODS-N/MODS region. With deep MOIRCS NIR images and IRAC images, we constructed the rest-frame UV-optical SEDs for ~130 LBGs. The contamination in IRAC images by neighboring objects is subtracted by using a PSF fitting software *GALFIT*. For this sample, we fitted the observed SEDs with population synthesis models. The comparisons of the distributions of parameters for our z~5 sample with those for z=2-3 samples in fixed rest-frame UV and optical ranges shows the increase of the stellar mass from z~5 to z=2-3 and that the z~5 galaxies are relatively younger than the z=2-3 galaxies. The star formation rate is also higher than that in z=2-3 galaxies. We also found that the stellar mass - star formation rate relation varies from z~5 to z=2-3. Our results imply that star formation history might rather be a periodic one.

1. Objective

Recent studies show the gradual increase of the stellar mass density with time. However, the studies on the stellar mass of galaxies at z>5 are restricted because the lack of sufficiently deep mid-IR data. With the advent of Spitzer, we can access the rest-frame optical wavelength, and thus, the stellar mass of galaxies at z~5. Yabe et al. (2009) explored the properties, especially stellar mass, of Lyman Break Galaxies (LBGs) by using a sample isolated in IRAC image with only optical and mid-IR data. In this work, we improve the observed SEDs with Subaru/S-Cam, MOIRCS and Spitzer/IRAC imaging data. The IRAC photometry for crowded objects is also improved by subtracting neighboring objects with *GALFIT*.

2. Data and Sample

In this work, we use 132 LBGs at z~5 in the GOODS-N/MODS (MOircs Deep Survey: ~120 arcmin^2) among LBGs discovered by Iwata et al. 2007.

Subaru/Suprime-Cam and MOIRCS
Magnitude limit (AB, 1.2''Φ, 5σ): V:28.2, Ic:26.9, z':26.6, J: 25.3(25.8), H: 24.7(25.0), K:25.0(25.5) in MODS deep (ultra deep)

Spitzer/IRAC
GOODS-N archival IRAC data
Magnitude limit (AB, 2.4''Φ, 3σ): 3.6μm:25.9, 4.5μm: 25.6

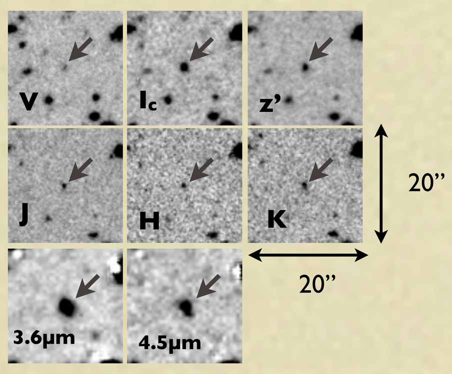

An example of the image of our sample

By using V, Ic, z' (Suprime-Cam), J, H, Ks (MOIRCS), 3.6μm, 4.5μm (IRAC) bands data, we derived optical-to-mid-IR SEDs for the sample. Limiting magnitude in each band is presented above and the image in each band of typical sample is also presented in the left.

3. IRAC contamination and population synthesis modeling

In some cases, target LBGs are seriously contaminated by neighboring objects in IRAC images. We subtracted neighboring objects in the IRAC images by using a PSF fitting software *GALFIT* (Peng et al. 2002) to avoid the severe contamination. An example is presented in the right figure.

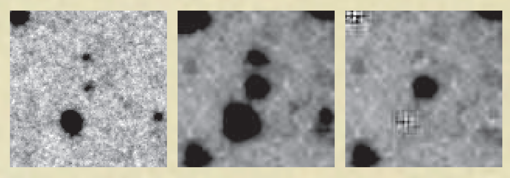

Example of the images of *GALFIT* process. From left to right: z'-band image, IRAC image (before *GALFIT*), and IRAC image (after *GALFIT*).

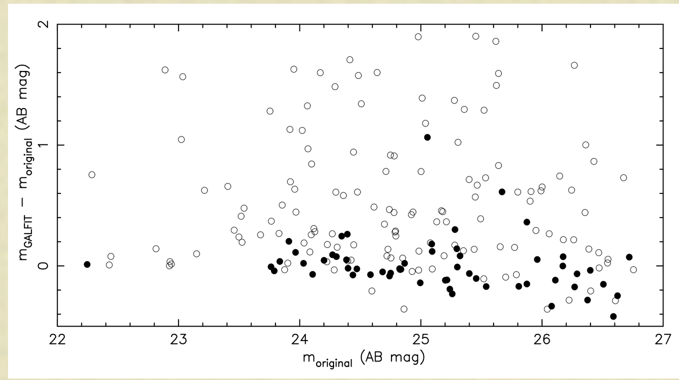

Differences between original magnitudes and magnitudes after *GALFIT* process in IRAC 3.6μm bands. Filled (open) circles indicate isolated (total) LBGs.

Yabe et al. (2009) chose isolate LBGs for their sample. Differences between original magnitudes and magnitudes after *GALFIT* process is presented in the left figure. It is clear that the differences for isolated LBGs are relatively small and almost Δm ~ 0 mag.

Note: Uncertainty in this *GALFIT* process is quantified by adding artificial objects and doing a similar procedure. The typical uncertainty is 5% - 30% depending objects' magnitude.

Population synthesis modeling is handled as shown in the right. Note that typical emission lines included in the model spectrum. We examine the effects of these model assumptions on the stellar mass and we found that the effects is ~0.3 dex at most.

- Bruzual & Charlot 2003
- Salpeter IMF (0.1 - 100 M_{sun})
- Constant Star Formation History
- 0.2 Z_{sun} model
- Calzetti extinction law
- Including Hα, Hβ, OII, OIII, NII emission lines
- Redshift of all objects is fixed to be z=4.8

4. Results

Comparing the observed SEDs with model SEDs, we infer the stellar properties of galaxies at z~5. In the bottom figures, examples of our fitting results are presented with the output parameters.

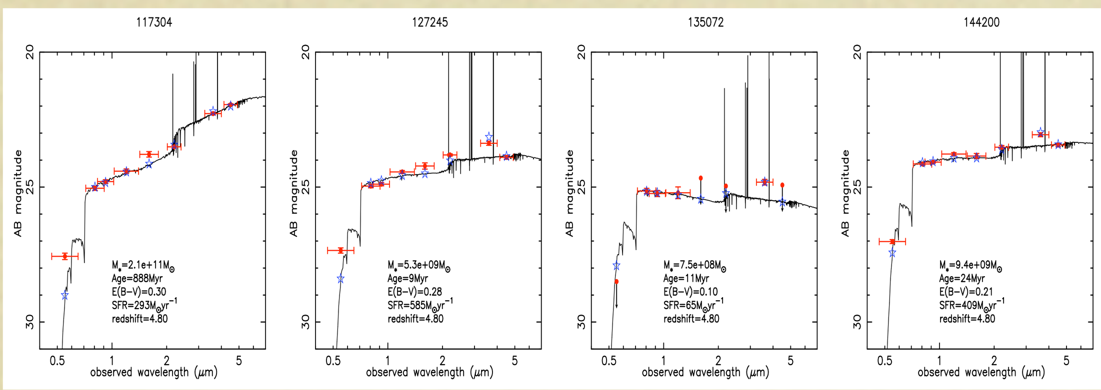

The best-fitted 0.2 Zsun, CSF models. The observed SEDs and the model SEDs are indicated by red points and blue points, respectively. The best-fitted spectra are presented with solid lines. The best-fitted parameters are also shown.

Distributions of the resulting output parameters are presented in the right figure. The median stellar mass, stellar age, color excess, and star formation rate are 3.5×10^9 M_{sun}, 25 Myr, 0.23 mag, and 140 M_{sun}/yr, respectively.

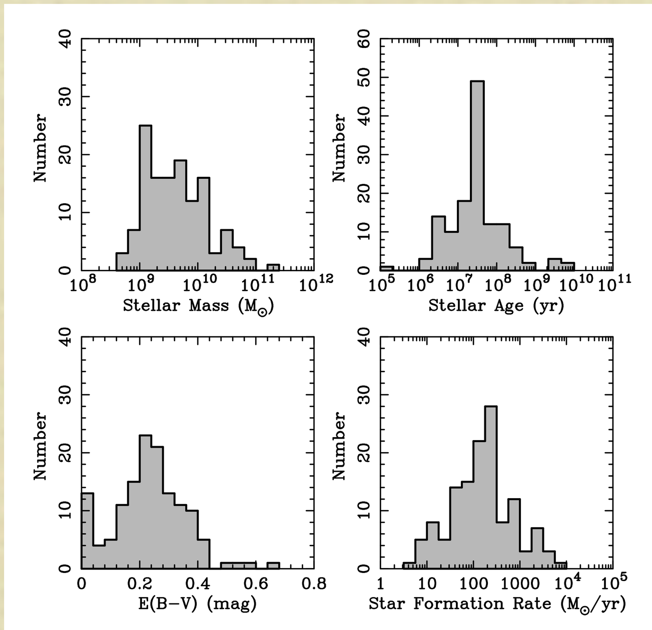

Distributions of best fitted parameters.

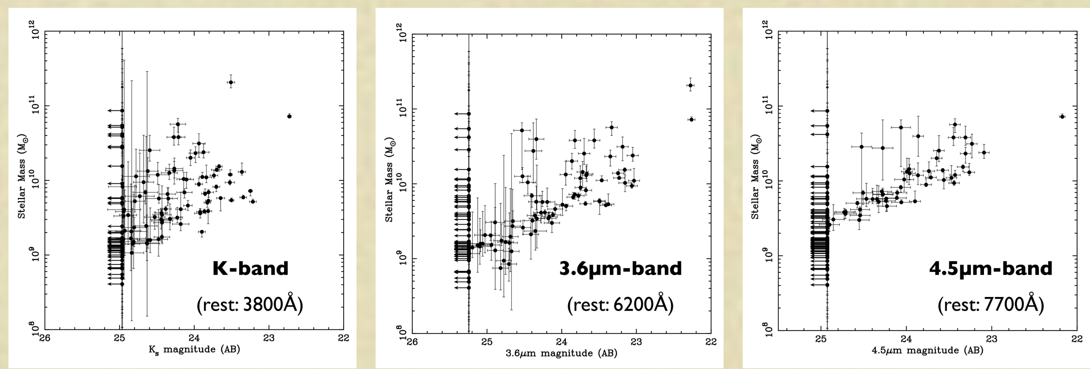

K_s, 3.6μm, and 4.5μm-band magnitudes vs. stellar mass. The rest-frame wavelength is calculated by assuming the redshift of z=4.8.

The stellar masses against magnitudes in Ks, 3.6μm, and 4.5μm-band are presented in above figure. The longer the wavelength is, the tighter is the correlation. The relation between stellar masses and z'-band magnitudes is presented in the right figure. There seems to be a week correlation between the two quantities.

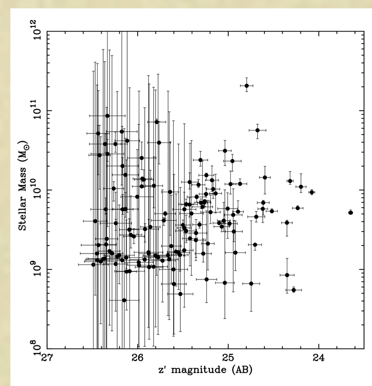

z'-band magnitude vs. stellar mass

5. Presence of Near-Infrared Data

For our sample, we examined how large the difference in the best-fitted parameters with and without NIR data is. The comparisons of the resulting parameters are presented in the right figure.

It is shown that there is no large difference between these parameters derived with and without NIR data, except for some outliers.

Caveats: The errors of NIR magnitudes are generally larger than those in the other bands and the weights of the NIR data to the SED fitting are relatively small. The results of the test might be caused by this effect.

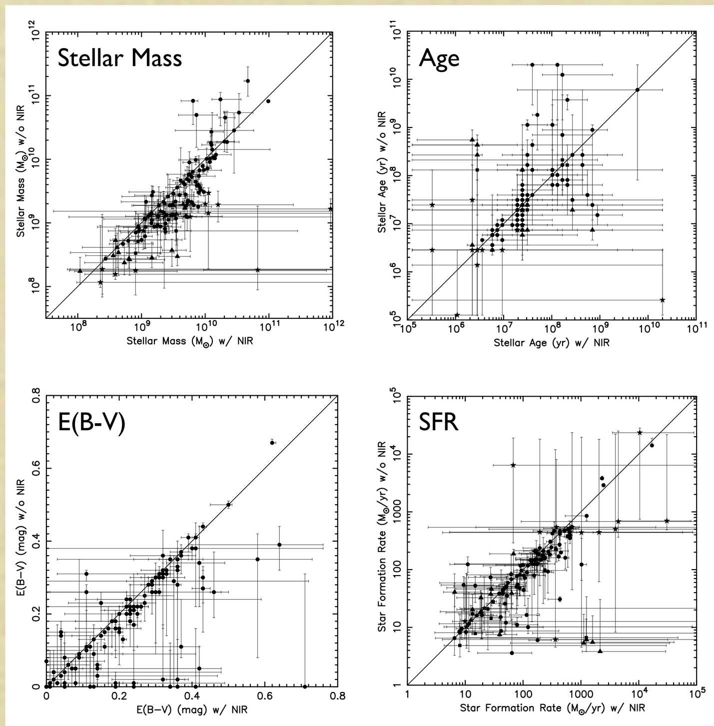

6. Comparisons of parameters with z=2-3 LBGs

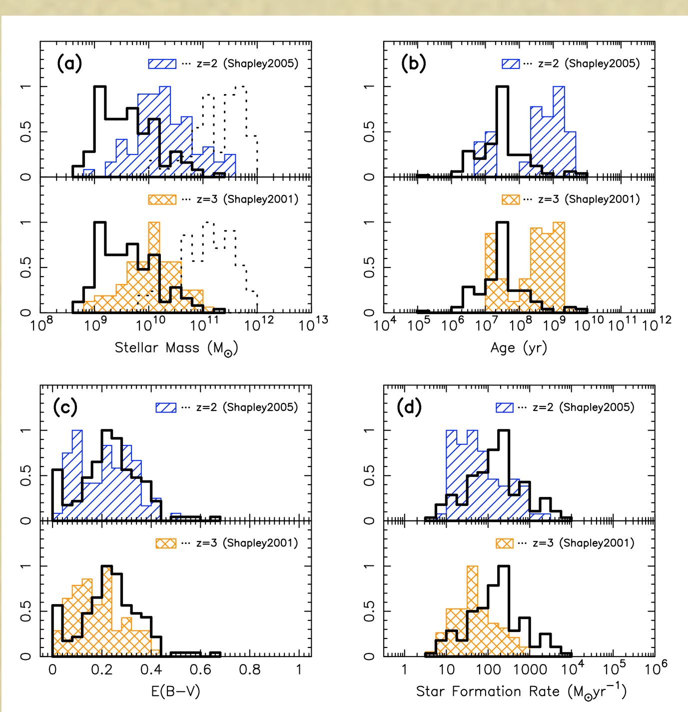

Distributions of best-fitted parameters for z~5 sample with those for z=3 sample from Shapley et al. (2001) (top panels) and z=2 sample from Shapley et al. (2005) (bottom panels). For comparison, peaks of the distributions are normalized to unity.

The distribution of the output parameters from the fitting of our sample is compared with those of z=2-3 sample in the figure below, where the histogram is normalized so that its peak value equals unity for comparison. For sample galaxies at z=2 and z=3, we use sample by Shapley et al. (2001) and Shapley et al. (2005), respectively.

Although the detailed algorithm of SED fitting procedure and assumptions are different from ours, both samples are fitted using population synthesis models by Bruzual & Charlot (2003) with a Salpeter IMF, constant star formation history, and the Calzetti et al. (2000) extinction law. For these z=2, 3, and 5 samples, the rest-frame UV and optical ranges are almost similar.

We found that the stellar mass of z~5 is smaller by a factor of 3-4 than that of z=2-3 galaxies and the age of z~5 galaxies is relatively younger than that of z=2-3. The star formation rate is higher than in z=2-3 by a factor of 2-3.

In the upper left panels of the figure above, the dotted lines indicate the distributions of stellar mass at z=2 and 3 assuming that each galaxy of our sample continues the star formation at the rate derived from the SED fitting until z=2 and 3. As a whole, the distribution shifts toward larger mass than observed at z=2 and 3. This implies that star formation rate may decrease from z~5 to z=2-3.

7. Star Formation History from z~5 to z=2-3

Relationship between stellar mass and star formation rate for z~5 LBGs is presented in the figure below and there seems to be a correlation between the two quantities. The correlations for z=0-2 galaxies are also presented in the figure.

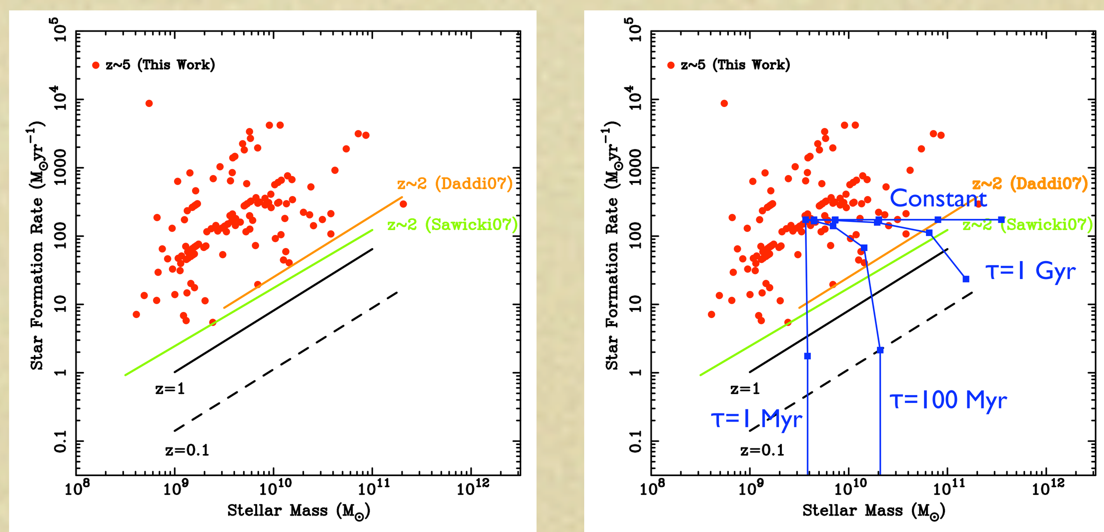

Left: Relation between stellar mass and star formation rate. Our sample at z~5 is indicated by red circles. z~2 samples are LBGs (green line) from Sawicki et al. 2007 and BzKs (orange line) from Daddi et al. 2007. z=0.1 (black solid line) and z=1 (black dashed line) are from Elbaz et al. 2007. ***Right***: Evolutionary tracks from z~5 to z~2 with various star formation scenario (constant, exp.-decay τ=1 Myr, 100 Myr, and 1 Gyr). The starting point indicates median values of both stellar mass and star formation rate. Blue squares indicate the time elapsed from the starting point Δt = 5 Myr, 20 Myr, 100 Myr, 400 Myr, and 2 Gyr.

It is shown that the relation evolves from z~5 to z~0. At a fixed stellar mass, the star formation rate decreases from z~5 to z~2 and to z~0.

In the figure above, evolutionary tracks from z~5 to z~2 with various star formation histories (constant, exponentially decay; τ=1 Myr, 100 Myr, and 1 Gyr).

If the constant star formation scenario is assumed, the expected relation at z~2 (~2 Gyr from z~5) appears to differ from that observed at z~2. Even if we assume other star formation histories, i.e. exponentially declining models, the predicted relation differs from the observations. Therefore, we conclude that the star formation rate decreases from z~5 to z~2 with episodic star formation.